Princeton Plasma Physics Laboratory

PPPL-4163

PPPL-4163

Reversed Shear Alvén Eigenmodes Associated with the Ellipticity and Triangularity Alfvén Gaps

G.J. Kramer and G-Y. Fu

June 2006

Prepared for the U.S. Department of Energy under Contract DE-AC02-76CH03073.

Princeton Plasma Physics Laboratory
Report Disclaimers

Full Legal Disclaimer

Trademark Disclaimer

PPPL Report Availability

Princeton Plasma Physics Laboratory

This report is posted on the U.S. Department of Energy's Princeton Plasma Physics Laboratory Publications and Reports web site in Fiscal Year 2006.

The home page for PPPL Reports and Publications is:

http://www.pppl.gov/pub_report/

Office of Scientific and Technical Information (OSTI):

Available electronically at: http://www.osti.gov/bridge.

Available for a processing fee to U.S. Department of Energy and its contractors, in paper from:

U.S. Department of Energy
Office of Scientific and Technical Information
P.O. Box 62
Oak Ridge, TN 37831-0062

Telephone: (865) 576-8401

Fax: (865) 576-5728

E-mail: reports@adonis.osti.gov

Reversed Shear Alfvén Eigenmodes Associated with the Ellipticity and Triangularity Alfvén Gaps.

G.J. Kramer* and G-Y. Fu

Princeton Plasma Physics Laboratories,

P.O.box 451, Princeton, New Jersey 08543

(Dated: May 11, 2006)

Abstract

Based on numerical simulations with the magnetohydrodynamic code NOVA, reversed shear Alfvén Eigenmodes (RSAE) associated with the ellipticity-induced and non-circular triangularity-induced Alfvén Eigenmode gaps were found. An analytical model for large aspect ratio plasmas confirms the existence of those modes with a pressure gradient threshold that agrees very well with the NOVA calculations. It is predicted that these higher gap RSAEs might be observed in existing large tokamaks in the early phase of reversed shear discharges when the minimum value of the magnetic safety factor is high (larger that two). Because the pressure-gradient threshold decreases with major radius these modes might readily show up in ITER plasmas.

*gkramer@pppl.gov

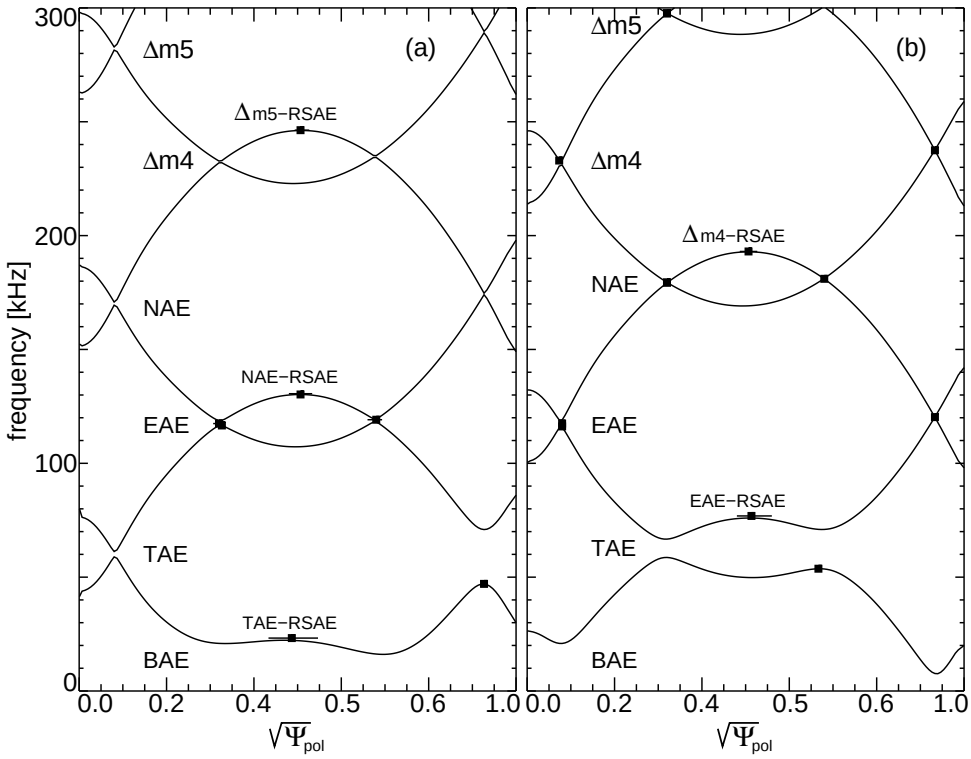

FIG. 1: Alfvén continua for a circular plasma cross section and aspect ratio of ten as a function of normalized flux coordinate ($\sqrt{\Psi_{\rm pol}} \approx r/a$). Eigenmode solutions as found with NOVA are indicated with the black squares. The pressure and q profiles for this simulation are shown in Fig. 2. In (a) $q_{\rm min} = 1.99$ was used while in (b) was $q_{\rm min} = 1.94$.

I. INTRODUCTION

A new class of Alfvén eigenmodes, the reversed shear Alfvén Eigenmodes (RSAE, sometimes called Alfvén Cascades) has been observed in several Tokamaks [1–8, 15] and explained theoretically [9–17]. Hallmarks of these modes are their localization at the minimum of the magnetic safety factor or q profile and a rapid up-chirping from about one-third to the Alfvén frequency when the minimum of the q profile decreases. The RSAE is related to the Torodicity-induced Alfvén Eigenmode (TAE) gap in the Alfvén continuum but there are other gaps as indicated in Fig. 1 and in this paper we show that similar RSAEs can be associated with higher frequency gaps at the shear reversal point. Below the TAE gap the Beta-induced Alfvén Eigenmode (BAE) gap exists. and is formed by finite pressure effects [18]. Above the TAE gap at about twice the TAE frequency, the Ellipticity-induced Alfvén

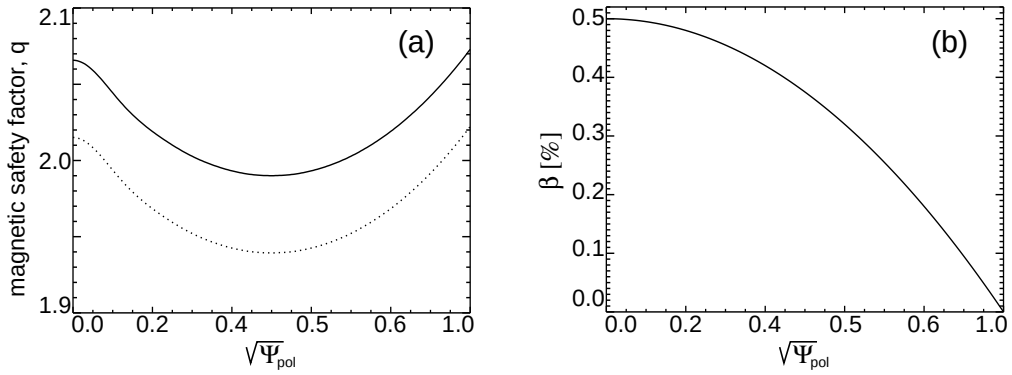

FIG. 2: Magnetic safety factor (a) and pressure profiles that were used to obtain the Alfvén continua of Fig. 1. The solid line in (a) was used for Fig. 1a while the dotted line was used for Fig. 1b.

Eigenmode (EAE) gap exists [19] which is formed by the coupling of poloidal harmonics m and $m+2$. It opens because of the plasma ellipticity. The third gap at three times the TAE frequency is the Non-circular triangularity-induced Alfvén Eigenmode (NAE) gap [20]. It is formed by the coupling of poloidal harmonics m and $m+3$, and opens due to the plasma triangularity. Alfvén eigenmodes have been observed in all these gaps [21–29]. Higher order gaps also exist with Δm4 and Δm5 (see Fig. 1) but modes in these gaps have not been observed experimentally.

The standard RSAE has a frequency just above the local maximum of the lowest branch of the Alfvén continuum at the minimum of the q profile ($q_{\min}$). When $q_{\min}$ decreases the frequency of the Alfvén continuum at $q_{\min}$ increases and the RSAE frequency increases until it reaches the TAE gap where it transforms into a TAE. Local maxima in the Alfvén continuum at $q_{\min}$ also exist in higher branches of the Alfvén continuum where modes similar to the RSAE are found in simulations performed with the non-variational magnetohydrodynamic (MHD) code NOVA [30, 31] as shown in Fig. 3 for RSAEs associated with the TAE, EAE, NAE, Δm4, and Δm5 gaps. Once found in the NOVA simulations, an analytical model was developed at large aspect ratio to confirm the validity of the numerical solutions. The analytic model is presented in section II, the numerical simulations in III, and a discussion of the optimal conditions for observing those modes is given in IV while conclusions are presented n section V.

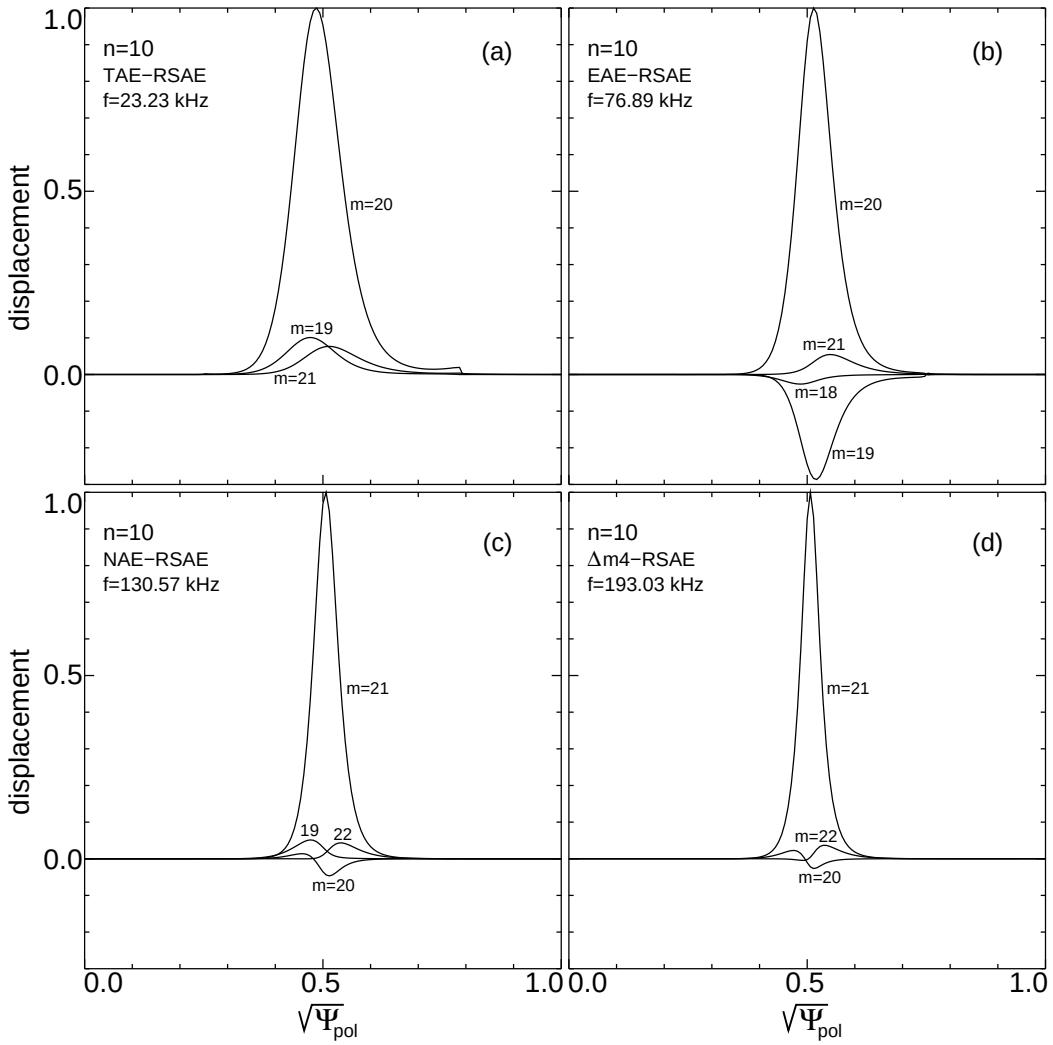

FIG. 3: RSAE solutions found with NOVA for modes associated with (a) the TAE gap, (b) the EAE gap, (c) the NAE gap, and (d) the Δm4 gap as a function of normalized flux coordinate ($\sqrt{\Psi_{\rm pol}} \approx r/a$). In those simulations an aspect ratio of 20 at the mode location was used with the pressure and q profiles shown in Fig. 2. For (a) and (c) $q_{\rm min}$ was taken to be 1.99 while for (b) and (d) a value of 1.94 was used.

II. ANALYTICAL MODEL

In Ref. [16] an analytical treatment was given of the RSAEs associated with the TAE gap where it was shown that a finite pressure gradient is contributing favorably to the mode existence; a finding that is supported by earlier NOVA simulations [13]. In Ref. [16] the linearized momentum equation was used together with a reduced MHD model for the shear

Alfvén waves in a low-beta plasma to obtain a criterion for the existence of the RSAEs associated with the TAE gap. The analytic criterion for the existence of RSAEs localized near $q_{\min}$ for large-aspect ratio finite-beta tokamaks with circular flux surfaces was derived in [10] and is given as:

$$Q > \frac{1}{4} \quad . \tag{1}$$

In various papers Q has been calculated with different assumptions for the plasma and/or fast-ion contributions [10, 12, 14, 16]. In Ref. [16] an expression for Q is obtained that includes terms up to quadratic in the pressure gradient:

$$Q = \frac{-mq_{\min}^2 k_m}{r_{\min}^2 q''_{\min}} \left(\frac{3\epsilon^2 - \alpha^2 + 2\epsilon\alpha(1 + 2(1 - q_{\min}^{-2})((2k_m q_{\min})^{-2} - 1))}{1 - (2k_m q_{\min})^2} \right) \tag{2}$$

with $\epsilon = r_{\min}/R_0$ the inverse aspect ratio (R_0 the major radius), $\Delta' = d\Delta/dr$ the derivative of the Shafranov shift, Δ, $\alpha = -(R_0 q_{\min}^2/B^2)dP/dr$, with P the plasma pressure and B the magnetic field strength, $q''_{\min} = d^2q/dr^2$ evaluated at $r_{\min}$, the location of $q_{\min}$ and $k_m = n - m/q_{\min}$ is the parallel wave number with n the toroidal and m the poloidal mode number.

The same expression can be used to investigate weather RSAEs associated with higher gaps can exist by using the appropriate values for k_m. For the conventional RSAEs associated with the TAE gap which appear experimentally as up-chirping modes when $q_{\min}$ decreases, k_m changes from zero at the rational q surface, m/n, to $-1/2q_{\mathrm{TAE}}$ when it transitions into a TAE at $q_{\mathrm{TAE}} = (m - 1/2)/n$. Therefore, Q is positive for RSAEs associated with the TAE gap under the condition for which Eq. 2 was derived: $\beta \sim O(\epsilon^2)$ which means that α is small. For RSAEs associated with the EAE, NAE, and higher order gaps k_m is less than minus one which means that the term: $1 - (2k_m q_{\min})^2$ is negative. The existence condition (Eq. 1) can only be fulfilled when the term: $3\epsilon^2 - \alpha^2 + 2\epsilon\alpha(1 + 2(1 - q_{\min}^{-2})((2k_m q_{\min})^{-2} - 1))$ is negative, i.e. when α exceeds a critical value: α_{crit}. In the limit of high poloidal mode numbers α_{crit} is proportional to the inverse aspect ratio:

$$\alpha_{\mathrm{crit}} = (b + \sqrt{b^2 + 3})\,\epsilon \tag{3}$$

with

$$b = 1 + 2(1 - 1/q_{\min}^2)((2k_m q_{\min})^{-2} - 1) \tag{4}$$

whereby expression in front of ϵ depends only on $q_{\min}$ and the toroidal and poloidal mode numbers of the RSAE. When we include the effect of finite poloidal mode numbers Eq. 3

changes to:

$$\alpha_{\rm crit} = (b + \sqrt{b^2 + c_m + 3})\,\epsilon \tag{5}$$

with

$$c_m = \frac{R_0^2 q''_{\rm min} k_m}{m}\left(\frac{1}{(2k_m q_{\rm min})^2} - 1\right) \tag{6}$$

where $\alpha_{\rm crit}$ now depends not only on $q_{\rm min}$, m, and n but also on the major radius and the shear rate near $q_{\rm min}$.

As an example we have evaluated Q (Eq. 2) as a function of α for a plasma with an inverse aspect ratio of 0.05 at the mode location and the following parameterizations of the pressure and q profiles (Fig. 2). The pressure was taken to be parabolic:

$$\beta(r) = P(r)/B^2 = (P_0/B^2)\,(1 - r^2) \tag{7}$$

with P_0 the central pressure, the q profile was given as:

$$q(r) = \frac{q_{\rm min}}{1 - ((r - r_{\rm min})/w_q)^2} \tag{8}$$

and the density profile was taken to be constant over the plasma radius.

In Fig. 4 we show Q as a function of α for a RSAE with mode numbers $(m, n) = (20, 10)$ at three values of $q_{\rm min}$ chosen in such a way that we obtain RSAEs associated with the TAE, EAE and NAE gaps. At $q_{\rm min} = 1.98$ the RSAE is associated with the TAE gap. This mode exists at zero α and because Q increases with α the mode continues to exist. The up-chirping RSAEs associated with the EAE, NAE, and higher gaps come only into existence when $\alpha_{\rm crit}$ is passed. From Fig. 4 it can be seen that $\alpha_{\rm crit}$ for RSAEs associated with the NAE gap (at $q_{\rm min} = 1.88$) is lower than the one for RSAEs associated with the EAE gap (at $q_{\rm min} = 1.92$). All these RSAEs exist just above the lower Alfvén continuum that encloses their respective gap as shown in Fig. 1.

Equation 2 was derived under the assumptions that $\beta \sim O(\epsilon^2)$ and for plasmas with circular cross sections. We will first first compare the predicted aspect ratio and $q_{\rm min}$ dependence of $\alpha_{\rm crit}$ with NOVA simulations for RSAEs associated with the NAE gap. This is followed by a study of the frequency behavior of various RSAEs as function of $q_{\rm min}$ for realistic plasma shapes and parameters.

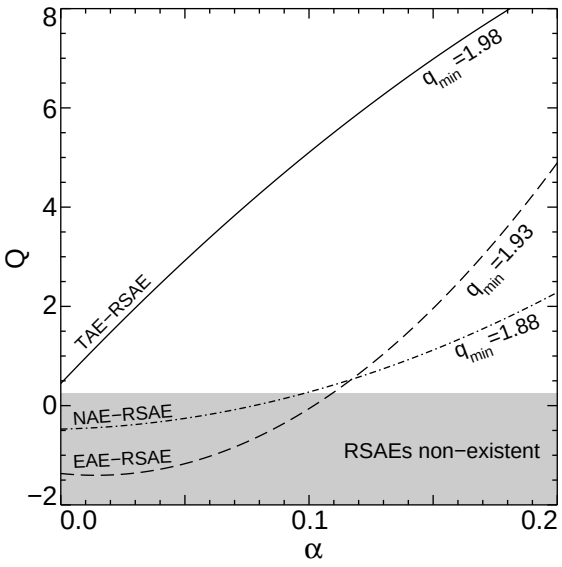

FIG. 4: Existence criterion for up-chirping RSAEs at the bottom of the gap with $n = 10$ and $m = 20$ associated with the TAE gap (solid curve) at $q_{\min} = 1.98$, the EAE gap (dashed curve) at $q_{\min} = 1.93$, and the NAE gap (dash-dotted curve) at $q_{\min} = 1.88$, for a toroidal plasma with $\epsilon = 0.05$ as a function of plasma pressure gradient. The modes don't exist below $Q = 0.25$ (gray area).

III. NUMERICAL SIMULATIONS

Theory predicts that above $\alpha_{\rm crit}$ RSAEs in gaps above the TAE gap can appear. For a large aspect ratio plasma with a circular cross section we have determined numerically with the NOVA code the $q_{\min}$ and aspect ratio dependencies and compared them with the results of Eqs. 3 and 5. A parabolic pressure profile (Eq. 7) was used together with a constant density profile and the q profile was parametrized according to Eq. 8.

For the $q_{\min}$ comparison we have used a model plasma with a circular cross section, a major radius, R_0, of 9 m, a minor radius, a, of 1 m. The minimum value of q was located at $r/a = 0.5$ and the width parameter was chosen to be $w_q = 2.5$. The critical α for the $n = 10$ mode was determined for RSAEs in the NAE gap. The RSAEs in the TAE and NAE gaps with $k_m < 0$ start at $q_{\min} = i/n$ with i a positive integer and n the toroidal mode number. In Fig. 5 we compare $\alpha_{\rm crit}$ calculated at $q = i/10 + 0.09$ for the analytical expression (Eq. 5) with values calculated by NOVA at $q = 0.99 + 0.5\,i$. From this figure it can be seen that $\alpha_{\rm crit}$ as calculated from NOVA agrees well with the analytical expression.

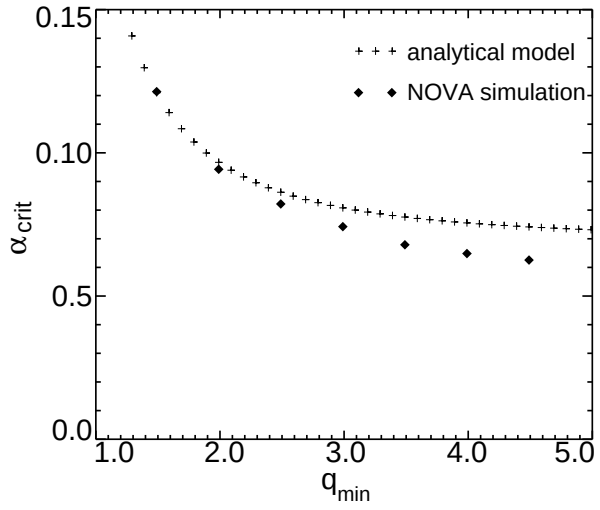

FIG. 5: The critical α above which RSAEs associated with the NAE gap can exist as function of the minimum magnetic safety factor. The crosses are from the analytical expression (Eq. 5) while the diamonds are determined from NOVA simulations. Details on the simulations are given in the text.

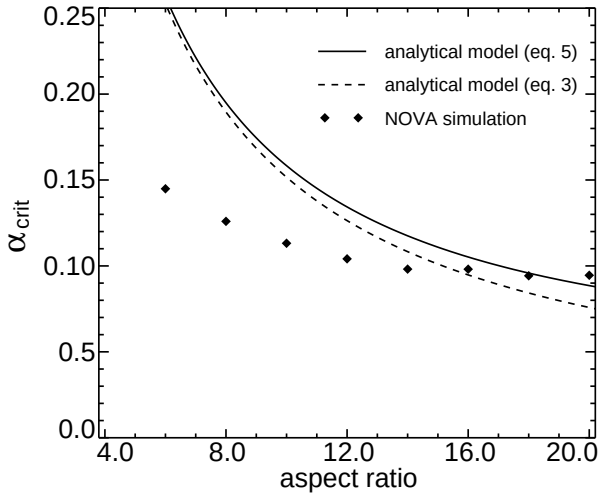

FIG. 6: The critical α above which RSAEs in the NAE gap can exists as function of aspect ratio. The dotted line is from Eq. 3 which does not include the correction for finite m while the solid line is for the analytical model which includes the finite m correction (Eq. 5) The diamonds are determined from NOVA simulations. Details on the simulations are given in the text.

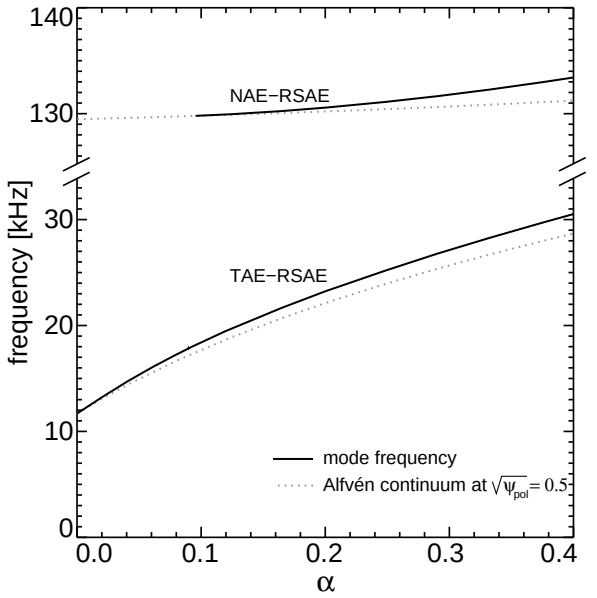

FIG. 7: Frequency behavior of $n = 10$ RSAEs associated with the TAE and NAE gaps as function of the pressure gradient at the mode location as a function of normalized flux coordinate ($\sqrt{\Psi_{\rm pol}} \approx r/a$). The TAE-RSAE exists in the absence of a pressure gradient while the NAE-RSAE has a critical pressure gradient above which it comes into existence. Both modes move away from the tip of the Alfvén continuum at $q_{\rm min}$ as the pressure gradient increases. Details on the simulations are given in the text.

A similar comparison was made for the variation in aspect ratio (Fig. 6). The aspect ratio was varied by changing the major radius between 3.0 and 10.0 m while keeping the minor radius fixed to 1.0 m and the mode location at r/a=0.5 whereby a circular plasma cross section was used. An $n = 10$ RSAE in the NAE gap was calculated with the following parameters for the q profile: $q_{\rm min}$ was fixed to 1.99, w_q was taken to be 2.5, and $q_{\rm min}$ was located at $r/a = 0.5$. The overall trend: $\alpha_{\rm crit}$, above which the mode exists, was found to increase in both the analytical theory and in the simulations with a decreasing aspect ratio (see Fig. 6) At large aspect ratios (large major radii) $\alpha_{\rm crit}$ from NOVA agree well with the ones from the analytical formula (Eq. 5) while at smaller aspect ratios (smaller major radii) the numerical values are lower that the analytical ones. This deviation is not so surprising because the theory was developed for large aspect ratio tori.

IV. FREQUENCY BEHAVIOR

The frequency behavior of the RSAE in the TAE and NAE gaps as function of α at the mode location is shown in Fig. 7 where it can be seen that the RSAE in the TAE gap exists even when α is zero. The RSAE in the NAE gap only comes into existence above $\alpha_{\rm crit}$ where it emerges from the tip of the Alfvén continuum at $q_{\rm min}$. When α increases both RSAEs move away from the tip of the Alfvén continuum indicating that the pressure gradient is contributing to the existence of these modes. For the calculations of Fig. 7 we have used the following parameters: $R_0 = 10$ m, $a = 1$ m, $q_{\rm min} = 1.99$, $r_{\rm min} = 0.5$, $w_q = 2.5$, a parabolic pressure profile, the adiabatic index of compression, $\gamma = 5/3$, and a constant density profile.

In reversed shear experiments, where RSAEs are observed, $q_{\rm min}$ is decreasing slowly. Therefore, we have calculated the frequency behavior of RSAEs associated with the TAE, EAE, and NAE gaps for two cases: first for a large aspect ratio torus with circular cross section, similar to the ones used in the comparison of the analytical theory with the simulations and second for a more realistic D-shaped plasma with an aspect ratio of three.

The frequency behavior of the $n = 10$ RSAEs associated with the TAE, EAE and NAE gaps as function of $q_{\rm min}$ is shown in Fig. 8 for a torus with and aspect ratio of ten ($R = 10$ m, $a = 1$ m) where the modes are located at $r/a = 0.5$. In this simulation we have again used a circular cross section, with a constant density profile and the q profile was parametrized according to Eq. 8 with $w_q = 2.5$, $r_{\rm min} = 0.5$ and $q_{\rm min}$ was varied from 2.0 to 1.85. Because the parabolic pressure profile was kept constant with $\beta(0) = 0.5\%$, α was decreasing in this scan from 0.20 at $q_{\rm min} = 2.0$ to 0.17 at $q_{\rm min} = 1.85$.

Eigenmode solutions from this simulation are shown in Fig. 3 for the points marked with diamonds in Fig. 8. The main poloidal harmonic of the RSAEs reflects the m number of the Alfvén continuum at $q_{\rm min}$ where the modes reside. From Fig. 8 it can be seen that both the BAE and TAE gaps are open because $\gamma = 5/3$ was used and the aspect ratio was finite. The EAE and NAE gaps are closed because of the circular plasma cross section. RSAEs associated with the TAE, EAE, and NAE gaps were found in the simulations and they all follow the Alfvén continuum frequency at the radius of $q_{\rm min}$ very accurately.

For studying RSAEs in a realistic case we have chosen a D-shaped plasma (elongation, $\kappa = 1.5$ and triangularity, $\delta = 0.2$) with a major radius of 3 m and minor radius of 1 m. The parameters for the q profile as given by Eq. 8 were: $w_q = 0.8$, $r_{\rm min} = 0.5$ and $q_{\rm min}$ varied

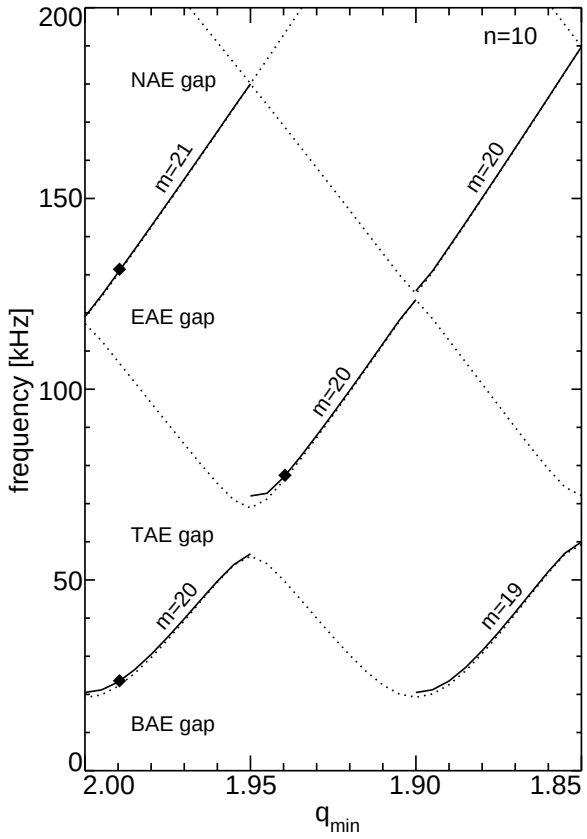

FIG. 8: (Solid lines) frequency behavior of $n = 10$ RSAEs associated with TAE, EAE, and NAE gaps as a function of the minimum value of the magnetic safety factor for a large aspect ratio plasma with circular cross section. The dominant poloidal harmonic, m, is indicated for the different branches. The RSAEs follow closely the frequency of the Alfvén continuum at $q_{\min}$ (dotted lines). Eigenmode solutions marked with diamonds are shown in Fig. 3. Details on the simulations are given in the text.

from 2.0 to 1.85 which led to variation in α from 0.12 at $q_{\min} = 2.0$ to 0.10 at $q_{\min} = 1.85$. The density profile was taken constant over the minor radius. In Fig. 9a the results of this $q_{\min}$-scan are shown where it can be seen that the BAE, TAE, EAE, and NAE gaps are all open due to $\gamma = 5/3$ for the BAE gap and to the plasma shaping for the other gaps. Only RSAEs associated with the TAE and NAE gaps were found in the simulations. No RSAEs associated with the EAE gap were found in these simulations. Only after an increase of α by more than a factor five the RSAE associated with the EAE gap appeared in the simulations indicating that the critical α is higher for RSAEs associated with the EAE gap than the RSAEs associated with the NAE gap. This is in agreement with the predictions from theory

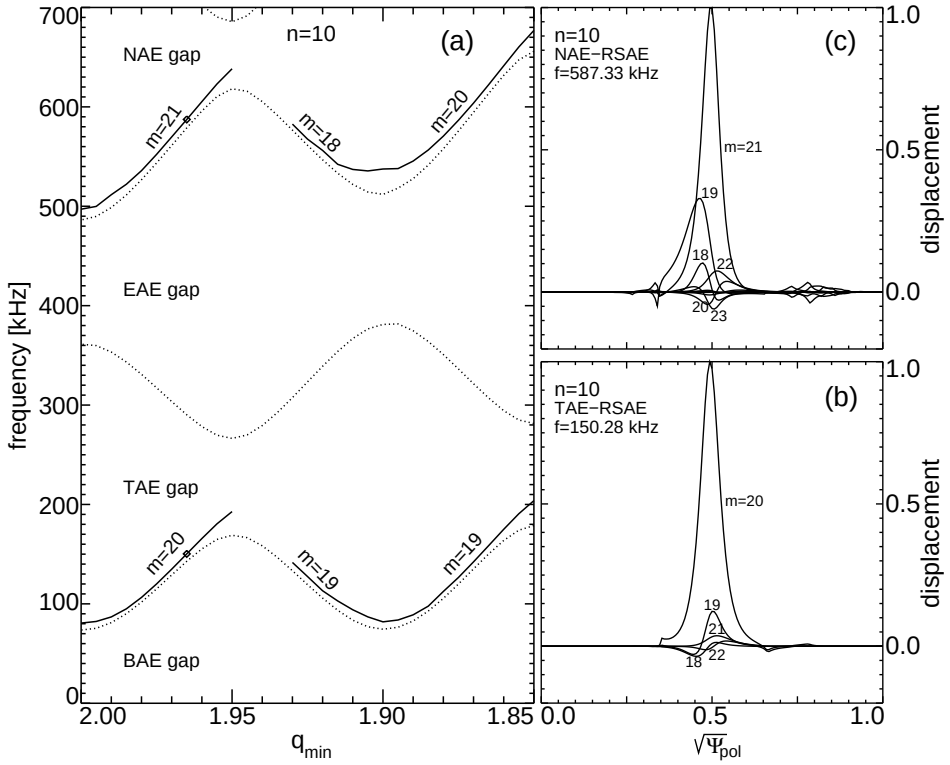

FIG. 9: (a) Frequency behavior (solid lines) of $n = 10$ RSAEs associated with TAE and NAE gaps as a function of the minimum value of the magnetic safety factor for a realistic D-shaped plasma with an aspect ratio of three. The dominant poloidal harmonic, m, is indicated for the different branches. The RSAEs follow closely the frequency of the Alfvén continuum at $q_{\rm min}$ (dotted lines). Eigenmode solution for the RSAE associated with the (b) TAE and (c) NAE gaps at $q_{\rm min} = 1.965$ as a function of normalized flux coordinate ($\sqrt{\Psi_{\rm pol}} \approx r/a$). The locations of those solutions is indicated with the diamonds in (a). Details on the simulations are given in the text.

(c.f. Fig. 4).

Typical RSAE solutions for the modes associated with the TAE and NAE gaps are shown in Fig. 9b and 9c, respectively. Apart from the increased number of side-band harmonics, the RSAE solution associated with the TAE gap in the realistic plasma shape of Fig. 9b is very similar to the large aspect ratio case of Fig. 3a. The RSAE solution associated with the NAE gap, however, differs somewhat from the large aspect ratio case. First, the $m = 19$ side-band harmonic is not small any more. Second, at $\sqrt{\Psi_{\rm pol}} \approx 0.8$ some coupling to a global NAE becomes apparent despite the fact that the Alfvén continuum is present between this part and the core-localized part of the mode. It has been found recently that intersections

of modes with the alfvén continuum do not necessary lead to high continuum damping rates [32]. Similar couplings have been observed previously in the TAE gap between global and core localized TAEs [33].

The best opportunity to observe RSAEs associated with the NAE gap is in the early stage of reversed shear discharges when $q_{\min}$ is high. This lowers α_{crit} above which the modes exists. For a circular plasma shape with an aspect ratio of three and a parabolic pressure profile α_{crit} at $q_{\min} = 3$ is about 0.25 and decreases to 0.22 at $q_{\min} = 5$. These numbers don't vary significantly for different toroidal mode numbers.

V. CONCLUSIONS

In numerical simulations with the NOVA code reversed shear Alfvén eigenmode solutions associated with with higher gaps, in particular the EAE, NAE, Δm4, and Δm5 gaps were found. All these modes reside at the magnetic shear reversal point and consist of one dominant poloidal harmonic. Analytical theory has corroborated the existence of those modes at large aspect ratios and predicted that the RSAEs in the gaps above the TAE gap only exist above a critical α, in contrast to the conventional RSAEs in the TAE gap which exist even at zero α. The theoretical predictions for α_{crit} compare well with values that were found with NOVA for plasmas with large aspect ratios, circular cross sections, and high poloidal mode numbers, the conditions under which the analytical theory was derived.

The frequency behavior of the RSAEs associated with the TAE, EAE, and NAE gaps was studied for two cases. For the large aspect ratio circular plasma cross section case, RSAEs were found to exist in the TAE, EAE, and NAE gaps and their frequencies follow the alfvén continuum frequency closely when $q_{\min}$ decreases. In the more realistic case, where we simulated the frequency behavior for a large tokamak with an aspect ratio of three and a D-shaped plasma cross section, only RSAEs associated with the TAE and NAE gaps were found when α was about 0.1. RSAEs associated with the EAE gap came only into existence when *alpha* was raised to above 0.5 indicating that α_{crit} for RSAEs associated with the EAE gap is much higher than for RSAEs associated with the NAE gap. This is in accordance with the analytical theory.

Depending on the values of $q_{\min}$ and R_0, RSAEs associated with the NAE gap can become unstable when α is in the range of 0.05 to 0.15. The best place to look for RSAEs associated

with the NAE gap is in Tokamaks with a large major radius such as JET, JT60U, and DIIID during the early phase of reversed shear discharges when $q_{\min}$ is still high ($q_{\min} > 2.0$). Because α is proportional to the major radius and the major radius of ITER is much larger than present day machines, α in ITER can therefore reach more easily values above $\alpha_{\rm crit}$ for the excitation of RSAEs associated with the NAE gap. Therefore, in ITER advanced plasma scenarios these modes might show up and influence the plasma performance.

Acknowledgments

We thank Dr. M. van Zeeland for for his suggestion to look for RSAEs associated with the EAE and NAE gaps in NOVA simulations. This work has been conducted under DOE Contract No. DE-AC02-76-CH0373.

[1] Y. Kusama, H. Kimura, T. Ozeki, M. Saigusa, G.J. Kramer, T. Oikawa, S. Moriyama, M. Nemoto, T. Fujita, K. Tobita, G.Y. Fu, R. Nazikian, and C.Z. Cheng, Nucl. Fusion **38** 1215 (1998).

[2] H. Kimura, Y. Kusama, M. Saigusa, G.J. Kramer, K. Tobita, M. Nemoto, T. Kondoh, T. Nishitani, O. Da Costa, T. Ozeki, T. Oikawa, S. Moriyama, A. Morioka, G.Y. Fu, C.Z. Cheng, and V.I. Afanas'ev, Nucl. Fusion **38** 1303 (1998).

[3] J.A. Snipes, A. Fasoli, P. Bonoli, S. Migliuolo, M. Porkolab, J.E. Rice, Y. Takase, and S.M. Wolfe, Plasma Phys. Contr. Fusion **42** 381 (2000).

[4] S.E. Sharapov, D. Testa, B. Alper, D.N. Borba, A. Fasoli, N.C. Hawkes, R.F. Heeter, M. Mantsinen, M.G. Von Hellermann, and contributors to the EFDA-JET work-programme, Phys. Lett. A **289** 127 (2001).

[5] R. Nazikian, G.J. Kramer, C.Z. Cheng, N.N. Gorelenkov, H.L. Berk, and S.E. Sharapov, Phys. Rev. Lett. **91** 125003 (2003).

[6] R. Nazikian, *et al.*, Proc. of the 20th IAEA international Conference on Fusion Energy, Portugal November 1-5 2004, EX/5-1.

[7] M.A. Van Zeeland, G.J. Kramer, R. Nazikian, H.L. Berk, T.N. Carlstrom, and W.M. Solomon, Plasma Phys. Contr. Fusion **47** L31 (2005).

[8] R. Nazikian, H.L. Berk, R.V. Budny, K. Burell, E. Doyle, R.J. Fonck, N.N. Gorelenkov, C. Holcomb, G.J. Kramer, J. Jayakumar, R. LaHaye, G.R. McKee, M. Makowski, W.A. Peebles, T.L. Rhodes, W. Solomon, E. Strait, M.A. VanZeeland, and L. Zeng, Phys. Rev. Lett. **96** 105006 (2006).

[9] A. Fukuyama, and T. Tohnai, Proceedings of the fifth IAEA Technical Committee Meeting on Alpha Particles in Fusion Research, Abingdon, 1997 edited by J. Jacquinot, B.E. Keen and G. Sadler, P. 81.

[10] H.L. Berk, D.N. Borba, B.N. Breizman, S.D. Pinches, and S.E. Sharapov Phys. Rev. Lett. **87** 185002 (2001).

[11] F. Zonca, S. Briguglio, L. Chen, S. Dettrick, G. Fogaccia, D. Testa, and G. Vlad, Phys. Plasmas **9** 4939 (2002).

[12] B.N. Breizman, H.L. Berk, M.S. Pekker, S.D. Pinches, and S.E. Sharapov Phys. Plasmas **10**

3649 (2003).

[13] G.J. Kramer, R. Nazikian, N.N. Gorelenkov, and C.Z. Cheng, Plasma Phys. Contr. Fusion **46** L23 (2004).

[14] B.N. Breizman, M.S. Pekker, S.E. Sharapov, and JET EFDA contributors, Phys. Plasmas **11** 4939 (2005).

[15] G.J. Kramer, R. Nazikian, B. Alper, M. de Baar, H.L. Berk, G-Y. Fu, N.N. Gorelenkov, G. McKee, S.D. Pinches, T.L. Rhodes, S.E. Sharapov, W.M. Solomon, M.A. Van Zeeland, and JET EFDA contributors Phys. Plasmas **13** 056104 (2006).

[16] G.Y. Fu and H.L. Berk, Phys. Plasmas **13** 052502 (2006).

[17] N.N. Gorelenkov, G.J. Kramer, and R. Nazikian, Interpretation of finite pressure gradient effects in the reversed shear Alfvén eigenmode theory. Submitted to Plasma Phys. Contr. Fusion.

[18] M. Chu, J.M. Greene, L.L. Lao, A.D. Turnbull, and M.S. Change Phys. Fluids B **4** 3713 (1992).

[19] R. Betti, and J.P. Freidberg, Phys. Fluids B **3** 1865 (1991).

[20] R. Betti, and J.P. Freidberg, Phys. Fluids B **4** 1465 (1992).

[21] K.L. Wong, R.J. Fonck, S.F. Paul, D.R. Roberts, E.D. Fredrickson, R. Nazikian, H.K. Park, M.G. Bell, N.L. Bretz, R.V. Budny, S. Cohen, G.W. Hammett, F.C. Jobes, D.M. Meade, S.S. Medley, D. Mueller, Y. Nagayama, D.K. Owens, and E.J. Synakowski, Phys. Rev. Lett. **66** 855 (1991).

[22] A.D. Turnbull, E.J. Strait, W.W. Heidbrink, M.S. Chu, H.H. Duong, J.M. Greene, L.L. Lao, T.S. Taylor, and S.J. Thompson, Phys. Fluids B **5** 2546 (1993).

[23] W.W. Heidbrink, E.J. Strait, M.S. Chu, and A.D. Turnbull, Phys. Rev. Lett. **71** 855 (1993).

[24] R. Nazikian, G.Y. Fu, S.H. Batha, M.G. Bell, R.E. Bell, R.V. Budny, C.E. Bush, Z. Chang, Y. Chen, C.Z. Cheng, D.S. Darrow, P.C. Efthimion, E.D. Fredrickson, N.N. Gorelenkov, B. Leblanc, F.M. Levinton, R. Majeski, E. Mazzucato, S.S. Medley, H.K. Park, M.P. Petrov, D.A. Spong, J.D. Strachan, E.J. Synakowski, G. Taylor, S. Von Goeler, R.B. White, K.L. Wong, and S.J. Zweben, Phys. Rev. Lett. **78** 2976 (1995).

[25] W.W. Heidbrink, A. Fasoli, D. Borba, and A. Jaun, Phys. Plasmas **4** 3663 (1997).

[26] G.J. Kramer, M. Saigusa, T. Ozeki, Y. Kusama, H. Kimura, T. Oikawa, K. Tobita, G.Y. Fu, and C.Z. Cheng, Phys. Rev. Lett. **80** 2594 (1998).

[27] K.L. Wong, Plasma Phys. Contr. Fusion **41** R1 (1999).

[28] G.J. Kramer, C.Z. Cheng, Y. Kusama, R. Nazikian, S. Takeji, and K. Tobita, Nucl. Fusion **41** 1135 (2001).

[29] G.J. Kramer, S.E. Sharapov, R. Nazikian, N.N. Gorelenkov, and R.V. Budny, Phys. Rev. Lett. **92** 015001 (2004).

[30] C.Z. Cheng and M.S. Chance, Journ. Comp. Phys. **71** 124 (1987).

[31] C.Z. Cheng, Phys. Rep. **211**, 1 (1992).

[32] N.N. Gorelenkov, Phys. Rev. Lett. **95** 265003 (2005).

[33] G.J. Kramer, C.Z. Cheng, G.Y. Fu, Y. Kusama, R. Nazikian, T. Ozeki, and K. Tobita, Phys. Rev. Lett. **83** 2961 (1999).

External Distribution

Plasma Research Laboratory, Australian National University, Australia
Professor I.R. Jones, Flinders University, Australia
Professor João Canalle, Instituto de Fisica DEQ/IF - UERJ, Brazil
Mr. Gerson O. Ludwig, Instituto Nacional de Pesquisas, Brazil
Dr. P.H. Sakanaka, Instituto Fisica, Brazil
The Librarian, Culham Science Center, England
Mrs. S.A. Hutchinson, JET Library, England
Professor M.N. Bussac, Ecole Polytechnique, France
Librarian, Max-Planck-Institut für Plasmaphysik, Germany
Jolan Moldvai, Reports Library, Hungarian Academy of Sciences, Central Research Institute for Physics, Hungary
Dr. P. Kaw, Institute for Plasma Research, India
Ms. P.J. Pathak, Librarian, Institute for Plasma Research, India
Dr. Pandji Triadyaksa, Fakultas MIPA Universitas Diponegoro, Indonesia
Professor Sami Cuperman, Plasma Physics Group, Tel Aviv University, Israel
Ms. Clelia De Palo, Associazione EURATOM-ENEA, Italy
Dr. G. Grosso, Instituto di Fisica del Plasma, Italy
Librarian, Naka Fusion Research Establishment, JAERI, Japan
Library, Laboratory for Complex Energy Processes, Institute for Advanced Study, Kyoto University, Japan
Research Information Center, National Institute for Fusion Science, Japan
Professor Toshitaka Idehara, Director, Research Center for Development of Far-Infrared Region, Fukui University, Japan
Dr. O. Mitarai, Kyushu Tokai University, Japan
Mr. Adefila Olumide, Ilorin, Kwara State, Nigeria
Dr. Jiangang Li, Institute of Plasma Physics, Chinese Academy of Sciences, People's Republic of China
Professor Yuping Huo, School of Physical Science and Technology, People's Republic of China
Library, Academia Sinica, Institute of Plasma Physics, People's Republic of China
Librarian, Institute of Physics, Chinese Academy of Sciences, People's Republic of China
Dr. S. Mirnov, TRINITI, Troitsk, Russian Federation, Russia
Dr. V.S. Strelkov, Kurchatov Institute, Russian Federation, Russia
Kazi Firoz, UPJS, Kosice, Slovakia
Professor Peter Lukac, Katedra Fyziky Plazmy MFF UK, Mlynska dolina F-2, Komenskeho Univerzita, SK-842 15 Bratislava, Slovakia
Dr. G.S. Lee, Korea Basic Science Institute, South Korea
Dr. Rasulkhozha S. Sharafiddinov, Theoretical Physics Division, Insitute of Nuclear Physics, Uzbekistan
Institute for Plasma Research, University of Maryland, USA
Librarian, Fusion Energy Division, Oak Ridge National Laboratory, USA
Librarian, Institute of Fusion Studies, University of Texas, USA
Librarian, Magnetic Fusion Program, Lawrence Livermore National Laboratory, USA
Library, General Atomics, USA
Plasma Physics Group, Fusion Energy Research Program, University of California at San Diego, USA
Plasma Physics Library, Columbia University, USA
Alkesh Punjabi, Center for Fusion Research and Training, Hampton University, USA
Dr. W.M. Stacey, Fusion Research Center, Georgia Institute of Technology, USA
Director, Research Division, OFES, Washington, D.C. 20585-1290

The Princeton Plasma Physics Laboratory is operated
by Princeton University under contract
with the U.S. Department of Energy.

Information Services
Princeton Plasma Physics Laboratory
P.O. Box 451
Princeton, NJ 08543

Phone: 609-243-2750
Fax: 609-243-2751
e-mail: pppl_info@pppl.gov
Internet Address: http://www.pppl.gov